

# SOME INVESTIGATIONS ON DIELECTRIC ROD WAVEGUIDE - PART II

BY V. SUBRAMANIAM

(Department of Electrical Communication Engineering, Indian Institute of Science, Bangalore-12)

Received on February 27, 1963

## ABSTRACT

Maximum power carrying capacity of a dielectric rod waveguide for  $\bar{\epsilon}_1=2.6$  and  $d=2.54$  cms has been calculated for  $H_{01}$ ,  $E_{01}$  and  $HE_{11}$  modes. For the  $HE_{11}$  mode the variation of the maximum power carrying capacity of the dielectric rod waveguide with its diameter has been studied. The radial decay of the electric field outside the dielectric rod waveguide and the guide wavelength  $\lambda_g$  of the waveguide have been experimentally measured at  $\lambda_0=3.2$  cms when the dielectric rod waveguide is excited in  $HE_{11}$  mode.

## FIELD COMPONENTS

The field components<sup>1</sup> are (Ref. Fig. 1) given below, omitting the time factor  $e^{i\omega t}$ .

$H_{01}$  mode: Inside the rod (medium 1),  $\rho \leq r$ ,

$$E_{\phi_1} = -BK_1 J'_0(K_1 \rho) e^{-\gamma_1 z},$$

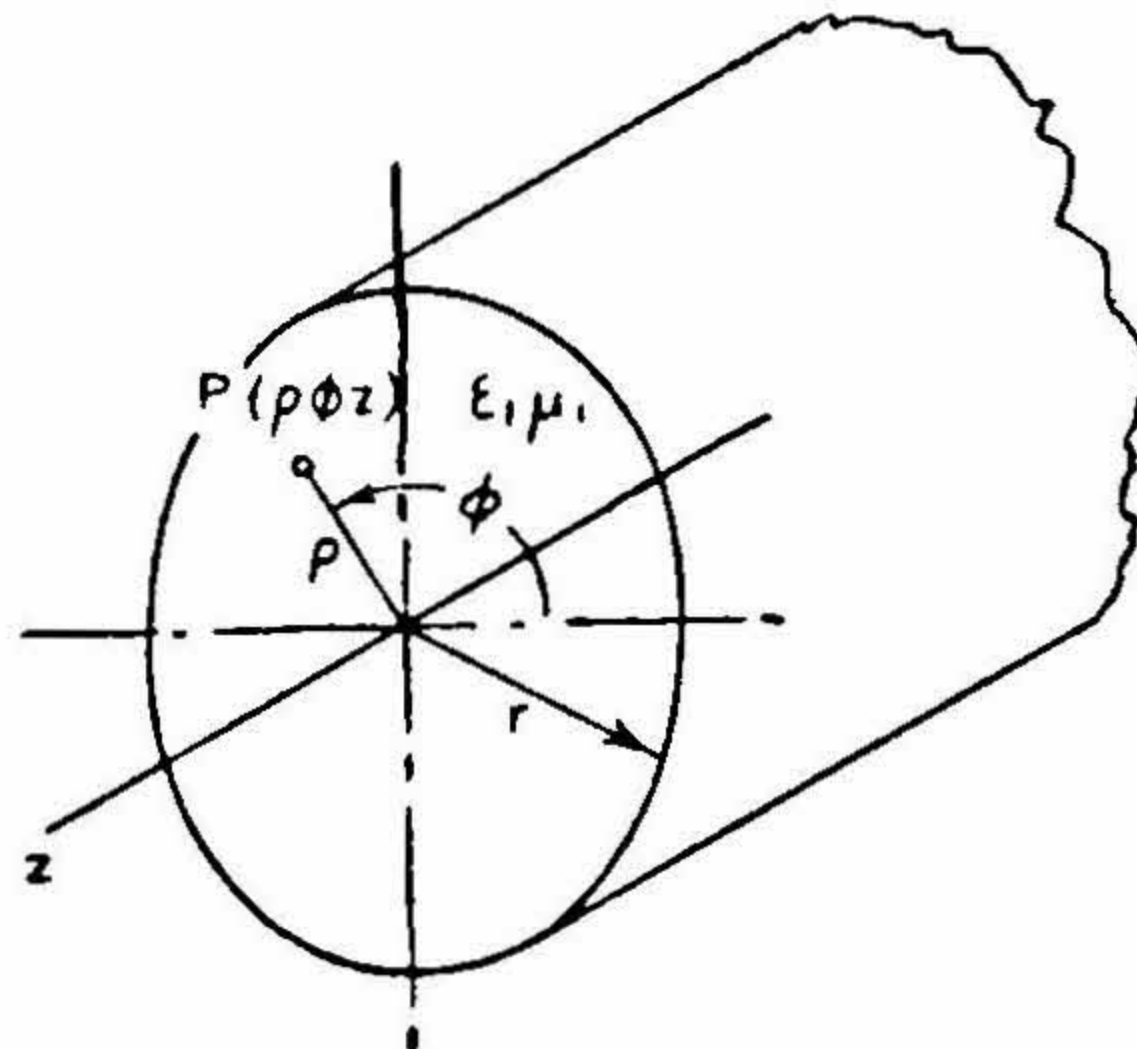


FIG. I

The Coordinate system  $(\rho, \phi, z)$  in the dielectric rod waveguide

$$\begin{aligned}
 H_{\rho_1} &= B \frac{\gamma_1 K_1}{i \omega \mu_1} J_0'(K_1 \rho) e^{-\gamma_1 z}, \\
 H_{z_1} &= -B \frac{K_1^2}{i \omega \mu_1} J_0(K_1 \rho) e^{-\gamma_1 z}.
 \end{aligned} \tag{1}$$

Outside the rod (medium 2),  $\rho \geq r$ ,

$$\begin{aligned}
 E_{\phi_2} &= -D K_2 H_0^{(1)'}(K_2 \rho) e^{-\gamma_2 z}, \\
 H_{\rho_2} &= D \frac{\gamma_2 K_2}{i \omega \mu_2} H_0^{(1)'}(K_2 \rho) e^{-\gamma_2 z}, \\
 H_{z_2} &= -D \frac{K_2^2}{i \omega \mu_2} H_0^{(1)}(K_2 \rho) e^{-\gamma_2 z}.
 \end{aligned} \tag{2}$$

$E_{01}$  mode: Inside the rod (medium 1),  $\rho \leq r$ ,

$$\begin{aligned}
 E_{\rho_1} &= -A \frac{\gamma_1 K_1}{i \omega \epsilon_1} J_0'(K_1 \rho) e^{-\gamma_1 z}, \\
 E_{z_1} &= A \frac{K_1^2}{i \omega \epsilon_1} J_0(K_1 \rho) e^{-\gamma_1 z}, \\
 H_{\phi_1} &= -A K_1 J_0'(K_1 \rho) e^{-\gamma_1 z}.
 \end{aligned} \tag{3}$$

Outside the rod (medium 2),  $\rho \geq r$ ,

$$\begin{aligned}
 E_{\rho_2} &= -C \frac{\gamma_2 K_2}{i \omega \epsilon_2} H_0^{(1)'}(K_2 \rho) e^{-\gamma_2 z}, \\
 E_{z_2} &= C \frac{K_2^2}{i \omega \epsilon_2} H_0^{(1)}(K_2 \rho) e^{-\gamma_2 z}, \\
 H_{\phi_2} &= -C K_2 H_0^{(1)'}(K_2 \rho) e^{-\gamma_2 z}.
 \end{aligned} \tag{4}$$

$HE_{11}$  mode: Inside the rod (medium 1),  $\rho \leq r$ ,

$$\begin{aligned}
 E_{\rho_1} &= -B \left[ \frac{1}{\rho} J_1(K_1 \rho) + \frac{b}{B} \cdot \frac{\gamma_1 K_1}{i \omega \epsilon_1} J_1'(K_1 \rho) \right] \sin \phi e^{-\gamma_1 z}, \\
 E_{\phi_1} &= -B \left[ K_1 J_1'(K_1 \rho) + \frac{b}{B} \cdot \frac{1}{\rho} \cdot \frac{\gamma_1}{i \omega \epsilon_1} J_1(K_1 \rho) \right] \cos \phi e^{-\gamma_1 z},
 \end{aligned}$$

$$\begin{aligned}
 E_{z_1} &= B \left[ \frac{b}{B} \cdot \frac{K_1^2}{i \omega \epsilon_1} J_1(K_1 \rho) \right] \sin \phi e^{-\gamma_1 z}, \\
 H_{\rho_1} &= B \left[ \frac{\gamma_1 K_1}{i \omega \mu_1} J_1'(K_1 \rho) + \frac{b}{B} \cdot \frac{1}{\rho} J_1(K_1 \rho) \right] \cos \phi e^{-\gamma_1 z}, \\
 H_{\phi_1} &= -B \left[ \frac{1}{\rho} \cdot \frac{\gamma_1}{i \omega \mu} J_1(K_1 \rho) + \frac{b}{B} K_1 J_1'(K_1 \rho) \right] \sin \phi e^{-\gamma_1 z}, \\
 H_{z_1} &= -B \left[ \frac{K_1^2}{i \omega \mu_1} J_1(K_1 \rho) \right] \cos \phi e^{-\gamma_1 z}. \tag{5}
 \end{aligned}$$

Outside the rod (medium 2),  $\rho \geq r$ ,

$$\begin{aligned}
 E_{\rho_2} &= -C \left[ \frac{1}{\rho} H_1^{(1)}(K_2 \rho) + \frac{c}{C} \cdot \frac{\gamma_2 K_2}{i \omega \epsilon_2} H_1^{(1)'}(K_2 \rho) \right] \sin \phi e^{-\gamma_2 z}, \\
 E_{\phi_2} &= -C \left[ K_2 H_1^{(1)'}(K_2 \rho) + \frac{c}{C} \cdot \frac{1}{\rho} \cdot \frac{\gamma_2}{i \omega \epsilon_2} H_1^{(1)}(K_2 \rho) \right] \cos \phi e^{-\gamma_2 z}, \\
 E_{z_2} &= C \left[ \frac{c}{C} \cdot \frac{K_2^2}{i \omega \epsilon_2} H_1^{(1)}(K_2 \rho) \right] \sin \phi e^{-\gamma_2 z}, \\
 H_{\rho_2} &= C \left[ \frac{\gamma_2 K_2}{i \omega \mu_2} H_1^{(1)'}(K_2 \rho) + \frac{c}{C} \cdot \frac{1}{\rho} H_1^{(1)}(K_2 \rho) \right] \cos \phi e^{-\gamma_2 z}, \\
 H_{\phi_2} &= -C \left[ \frac{1}{\rho} \cdot \frac{\gamma_2}{i \omega \mu_2} H_1^{(1)}(K_2 \rho) + \frac{c}{C} \cdot K_2 H_1^{(1)'}(K_2 \rho) \right] \sin \phi e^{-\gamma_2 z}, \\
 H_{z_2} &= -C \left[ \frac{K_2^2}{i \omega \mu_2} H_1^{(1)}(K_2 \rho) \right] \cos \phi e^{-\gamma_2 z}. \tag{6}
 \end{aligned}$$

In the equations [1] to [6],

$K_1$  = radial propagation constant inside the rod

$K_2$  = radial propagation constant outside the rod

$\gamma_1 = \sqrt{K_1^2 - \omega^2 \mu_1 \epsilon_1}$  = axial propagation constant inside the rod

$\gamma_2 = \sqrt{K_2^2 - \omega^2 \mu_2 \epsilon_2}$  = axial propagation constant outside the rod

$\mu_1, \mu_2$  are the permeabilities of the media (1) and (2)

$\epsilon_1, \epsilon_2$  are the permittivities of the media (1) and (2)

$A, B, C, D, b$  and  $c$  are constants.

For the same mode to propagate inside and outside the dielectric rod waveguide,

$$\gamma_1 = \gamma_2 = \gamma$$

which means that  $K_1$  and  $K_2$  must satisfy the equation

$$x_1^2 + \left(\frac{x_2}{i}\right)^2 = \left(\frac{\pi d}{\lambda_0}\right)^2 (\bar{\epsilon}_1 - 1), \quad [7]$$

where

$$x_1 = K_1 r,$$

$$x_2 = K_2 r,$$

$$d = 2r = \text{diameter of the rod},$$

$$\bar{\epsilon}_1 = \text{relative dielectric constant of medium (1)},$$

$$\lambda_0 = \text{free space wavelength of the waves.}$$

#### CHARACTERISTIC EQUATION

$H_{01}$  mode: The characteristic equation for this mode is

$$x_1 \frac{J_0(x_1)}{J'_0(x_1)} = x_2 \frac{H_0^{(1)}(x_2)}{H_0^{(1)'}(x_2)} \quad [8]$$

Equations [7] and [8] are to be simultaneously solved for  $x_1$  and  $x_2$ .  $x_1$  and  $x_2$  are obtained graphically, as shown in Fig. 2, for perspex rod of  $\bar{\epsilon}_1 = 2.6$  and diameter  $d = 2.54$  cms.  $x_1$  and  $x_2$  are found to be

$$x_1 = 2.78, \quad x_2 = 1.486 i$$

$$K_1 = 2.189, \quad K_2 = 1.173 i$$

and

$$\gamma = 2.285 i. \quad [9]$$

The values of  $K_1$ ,  $K_2$  and  $\gamma$  are expressed per cm.

$E_{01}$  mode: The characteristic equation of this mode is

$$x_1 \frac{J_0(x_1)}{J'_0(x_1)} = \bar{\epsilon}_1 x_2 \frac{H_0^{(1)}(x_2)}{H_0^{(1)'}(x_2)}. \quad [10]$$

For  $\bar{\epsilon}_1 = 2.6$  and  $d = 2.54$  cms.,  $x_1$  and  $x_2$  satisfying the equations [10] and [7] simultaneously, obtained from the Fig. 2 are

$$x_1 = 2.95, \quad x_2 = 1.11 i$$

$$K_1 = 2.32, \quad K_2 = 0.87 i$$

and

$$\gamma = 2.15 i \quad [11]$$

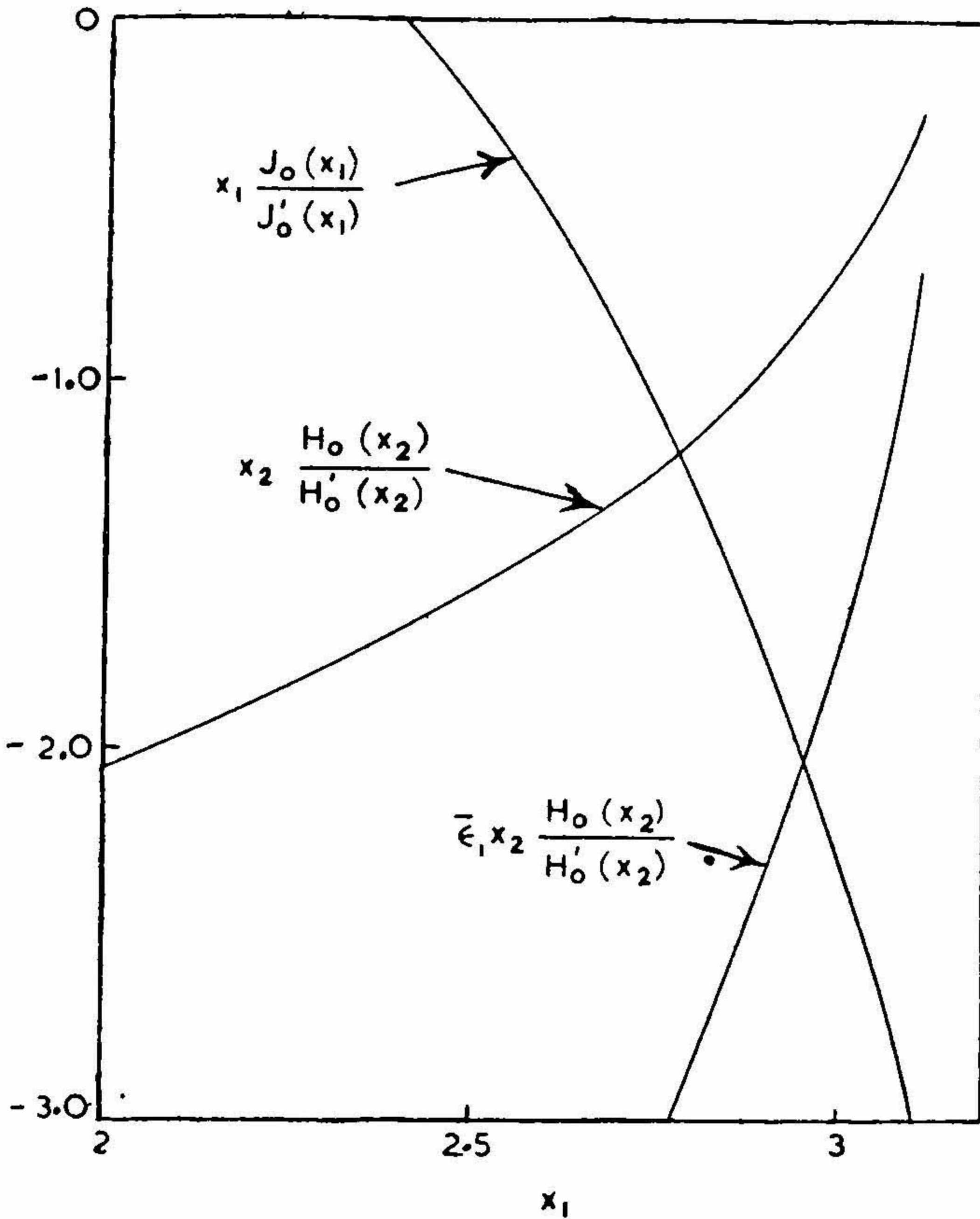


FIG. II

Graphical solution of the characteristic equations [8] and [10] for  $d/\lambda_0=0.8$ ,  $\bar{\epsilon}_1=2.6$  and  $\lambda_0=3.2$  cms.

$H_0(x_2)$  and  $H_0'(x_2)$  in the graph are Hankel functions of the 1st kind.

$HE_{11}$  mode: For this mode  $x_1$  and  $x_2$  must satisfy the equation [7] and the following equation.

$$\left[ \frac{1}{x_1} \cdot \frac{J_1'(x_1)}{J_1(x_1)} - \frac{1}{x_2} \cdot \frac{H_1^{(1)'}(x_2)}{H_1^{(1)}(x_2)} \right] \left[ \frac{\bar{\epsilon}_1}{x_1} \cdot \frac{J_1'(x_1)}{J_1(x_1)} - \frac{1}{x_2} \cdot \frac{H_1^{(1)'}(x_2)}{H_1^{(1)}(x_2)} \right] = \frac{(x_1^2 - x_2^2)(x_1^2 - \bar{\epsilon}_1 x_2^2)}{x_1^4 x_2^4} \quad [12]$$

$x_1$  and  $x_2$  are obtained graphically<sup>2</sup> for  $\bar{\epsilon}_1 = 2.6$  and for various values of  $d$ .  
For  $d = 2.54$  cms.,

$$x_1 = 1.995, \quad x_2 = 2.438 i$$

$$K_1 = 1.57, \quad K_2 = 1.92 i$$

and 
$$\gamma = 2.75 i. \quad [13]$$

### MAXIMUM POWER CARRYING CAPACITY

In the case of a dielectric rod waveguide, the electromagnetic field exists inside as well as outside the waveguide. The maximum power carrying capacity of the waveguide is determined by the breakdown field strength of the medium 1 or that of the medium 2, whichever is lower. Since air breaks down earlier than solid dielectrics, if the surrounding medium is air, the maximum permissible field strength in medium 2 is  $\hat{E}$ , the break down field strength for air.

*H<sub>01</sub> mode*: The constants  $B$  and  $D$  in the field equations [1] and [2] are expressed in terms of the break down field strength of air. The only electric field component outside the rod,  $E_{\phi_2}$  is maximum at the surface of the rod where  $\rho = r = 1.27$  cms

$$\therefore D = i \frac{\hat{E}}{0.2102}. \quad [14]$$

At the boundary 
$$\rho = r, \quad E_{\phi_1} = E_{\phi_2}$$

which yields 
$$B = D \frac{K_2}{K_1} \cdot \frac{H_0^{(1)'}(K_2 r)}{J_0'(K_1 r)} = 1.09 \hat{E}. \quad [15]$$

The mean value of the power flow along Z-axis inside the rod is

$$P_{z_i} = \frac{1}{2} \text{Re} \int_{\phi=0}^{2\pi} \int_{\rho=0}^r -E_{\phi_1} H_{\rho_1}^* \rho d\rho d\phi$$

$$= \frac{1}{2} \text{Re} \left[ - \frac{2\pi B B^* K_1^2 \gamma_1^*}{i \omega \mu_1} \int_{\rho=0}^r \rho J_1^2(K_1 \rho) d\rho \right]$$

The integral has been evaluated by numerical methods. Substituting the values from [9] and [14].

$$P_{z_i} = 0.0116 \hat{E}^2. \quad [16]$$

The mean value of the power flow along Z-axis outside the rod is

$$\begin{aligned}
 P_{z_0} &= \frac{1}{2} \operatorname{Re} \int_{\phi=0}^{2\pi} \int_{\rho=r}^{\infty} -E_{\phi_2} H_{\rho_2}^* \rho d\rho d\phi \\
 &= \frac{1}{2} \operatorname{Re} \left[ -\frac{2\pi D D^* K_2 K_2^* \gamma_2^*}{i\omega\mu_2} \int_{\rho=r}^{\infty} \rho H_1^{(1)}(K_2\rho) H_1^{(2)}(K_2^*\rho) d\rho \right] \\
 &= 0.0048 \hat{E}^2.
 \end{aligned} \tag{17}$$

Adding [16] and [17], the maximum power flow is

$$P_z = P_{z_i} + P_{z_0} = 0.0164 \hat{E}^2.$$

For air at microwave frequencies at normal temperature and pressure, the breakdown field strength<sup>3</sup> is  $\hat{E} = 2.9 \times 10^9$  V/m. Hence,

$$P_2 = 13.87 \text{ Megawatts.} \tag{18}$$

*E<sub>01</sub> mode*: Considering the field components given in the equation [4], both radial and axial electric field components outside the rod are maximum at  $\rho = r$ . The maximum value of the electric field is

$$E = \sqrt{|E_{\rho_2}|^2 + |E_{z_2}|^2}.$$

But, in this case, the radial and axial field components are in time quadrature so that the maximum value of the resultant field is the maximum value of the larger component. Hence, the maximum resultant electric field is

$$\hat{E} = -i115C, \quad C = i[\hat{E}/115]. \tag{19}$$

At the boundary  $\rho = r$ ,  $E_{z_1} = E_{z_2}$

$$A = C \frac{K_2^2}{K_1^2} \frac{\epsilon_1}{\epsilon_2} \frac{H_0^{(1)}(K_2 r)}{J_0(K_1 r)} = 0.003 \hat{E} \tag{20}$$

The mean value of the power flow along the z-axis inside the rod waveguide is

$$\begin{aligned}
 P_{z_i} &= \frac{1}{2} \operatorname{Re} \int_{\phi=0}^{2\pi} \int_{\rho=0}^r E_{\rho_1} H_{\phi_1}^* \rho d\rho d\phi \\
 &= \frac{1}{2} \operatorname{Re} \left[ \frac{2\pi A A^* K_1^2 \gamma_1}{i\omega\epsilon_1} \int_{\rho=0}^r \rho J_1^2(K_1\rho) d\rho \right] \\
 &= 0.005 \hat{E}^2.
 \end{aligned} \tag{21}$$

The mean value of the power flow along Z-axis outside the rod waveguide is

$$\begin{aligned}
 P_{z_0} &= \frac{1}{2} \operatorname{Re} \int_{\phi=0}^{2\pi} \int_{\rho=r}^{\infty} E_{\rho_2} H_{\phi_2}^* \rho d\rho d\phi \\
 &= \frac{1}{2} \operatorname{Re} \left[ \frac{C C^* \gamma_2 K_2 K_2^*}{i \omega \epsilon_2} 2\pi \int_{\rho=r}^{\infty} \rho H_1^{(1)}(K_2 \rho) H_1^{(2)}(K_2^* \rho) d\rho \right] \\
 &= 0.016 \hat{E}^2.
 \end{aligned} \tag{22}$$

Adding [21] and [22], the maximum power flow is

$$P_z = P_{z_i} + P_{z_0} = 17.76 \text{ megawatts.}$$

*HE<sub>11</sub> mode*: The instantaneous absolute values of the electric field components outside at the surface of the rod, for  $d = 2.54$  cms and  $\bar{\epsilon}_1 = 2.6$ , obtained from the equations [6] are

$$\begin{aligned}
 E_{\rho_2} &= 0.1402 C \sin \phi \sin \omega t, \\
 E_{\phi_2} &= 0.0552 C \cos \phi \sin \omega t, \\
 E_{z_2} &= 0.0888 C \sin \phi \cos \omega t.
 \end{aligned} \tag{23}$$

The instantaneous absolute value of the resultant electric field intensity at the surface outside the rod is

$$E = \sqrt{|E_{\rho_2}|^2 + |E_{\phi_2}|^2 + |E_{z_2}|^2}$$

This is maximum when  $\omega t = \pi/2$  and  $\phi = \pi/2$

$$\hat{E} = 0.1402 C \quad \text{or} \quad C = \hat{E}/0.1402 \tag{24}$$

Applying the boundary conditions at  $\rho = r$  yields<sup>2</sup>

$$\begin{aligned}
 \frac{b}{B} &= \frac{\gamma \epsilon_1}{i \omega \mu_1} \cdot \frac{x_1^2 - x_2^2}{x_1^2 x_2^2} \left[ \frac{\epsilon_1}{x_1} \cdot \frac{J_1'(x_1)}{J_1(x_1)} - \frac{\epsilon_2}{x_2} \cdot \frac{H_1^{(1)'}(x_2)}{H_1^{(1)}(x_2)} \right]^{-1}, \\
 \frac{c}{C} &= \frac{\gamma \epsilon_2}{i \omega \mu_2} \cdot \frac{x_1^2 - x_2^2}{x_1^2 x_2^2} \left[ \frac{\epsilon_1}{x_1} \cdot \frac{J_1'(x_1)}{J_1(x_1)} - \frac{\epsilon_2}{x_2} \cdot \frac{H_1^{(1)'}(x_2)}{H_1^{(1)}(x_2)} \right]^{-1}, \\
 B &= C \frac{K_2^2}{K_1^2} \cdot \frac{H_1^{(1)}(K_2 r)}{J_1(K_1 r)} = \frac{\hat{E}}{1.0686}.
 \end{aligned} \tag{25}$$

The mean value of the power flow<sup>2</sup> inside the dielectric rod waveguide along the Z-axis is

$$\begin{aligned}
 P_{z_i} = B^2 & \left[ \frac{b}{B} \pi K_1 \left( 1 - \frac{\gamma_1^2}{\omega^2 \mu_1 \epsilon_1} \right) \int_{\rho=0}^r J_0(K_1 \rho) J_1(K_1 \rho) d\rho \right. \\
 & - \frac{\pi \gamma_1 K_1}{i \omega} \left( \frac{1}{\mu_1} + \frac{b^2}{B^2} \cdot \frac{1}{\epsilon_1} \right) \int_{\rho=0}^r J_0(K_1 \rho) J_1(K_1 \rho) d\rho \\
 & + \frac{\pi \gamma_1}{i \omega} \left( \frac{1}{\mu_1} + \frac{b^2}{B^2} \cdot \frac{1}{\epsilon_1} \right) \int_{\rho=0}^r \frac{1}{\rho} J_1^2(K_1 \rho) d\rho \\
 & - \frac{b}{B} \pi \left( 1 - \frac{\gamma_1^2}{\omega^2 \mu_1 \epsilon_1} \right) \int_{\rho=0}^r \frac{1}{\rho} J_1^2(K_1 \rho) d\rho \\
 & \left. + \frac{\pi \gamma_1 K_1^2}{2 i \omega} \left( \frac{1}{\mu_1} + \frac{b^2}{B^2} \cdot \frac{1}{\epsilon_1} \right) \int_{\rho=0}^r \rho J_0^2(K_1 \rho) d\rho \right] \\
 & = 0.00119 \hat{E}^2. \tag{26}
 \end{aligned}$$

The mean value of the power flow outside the dielectric rod waveguide along Z-axi is

$$\begin{aligned}
 P_{z_0} = C^2 & \left[ \frac{c}{C} \pi K_2 \left( 1 - \frac{\gamma_2^2}{\omega^2 \mu_2 \epsilon_2} \right) \int_{\rho=r}^{\infty} H_0^{(1)}(K_2 \rho) H_1^{(1)}(K_2 \rho) d\rho \right. \\
 & - \frac{\pi \gamma_2 K_2}{i \omega} \left( \frac{1}{\mu_2} + \frac{c^2}{C^2} \cdot \frac{1}{\epsilon_2} \right) \int_{\rho=r}^{\infty} H_0^{(1)}(K_2 \rho) H_1^{(1)}(K_2 \rho) d\rho \\
 & + \frac{\pi \gamma_2}{i \omega} \left( \frac{1}{\mu_2} + \frac{c^2}{C^2} \cdot \frac{1}{\epsilon_2} \right) \int_{\rho=r}^{\infty} \frac{1}{\rho} [H_1^{(1)}(K_2 \rho)]^2 d\rho \\
 & - \frac{c}{C} \pi \left( 1 - \frac{\gamma_2^2}{\omega^2 \mu_2 \epsilon_2} \right) \int_{\rho=r}^{\infty} \frac{1}{\rho} [H_1^{(1)}(K_2 \rho)]^2 d\rho \\
 & \left. + \frac{\pi \gamma_2 K_2}{2 i \omega} \left( \frac{1}{\mu_2} + \frac{c^2}{C^2} \cdot \frac{1}{\epsilon_2} \right) \int_{\rho=r}^{\infty} \rho [H_0^{(1)}(K_2 \rho)]^2 d\rho \right] \\
 & = 0.00115 \hat{E}^2. \tag{27}
 \end{aligned}$$

Adding [26] and [27], the maximum power flow is

$$P_2 = P_{z_i} + P_{z_0} = 11 \text{ Megawatts.}$$

The maximum power flow for perspex rod ( $\bar{\epsilon}_1 = 2.6$ ), excited in the hybrid mode, of various diameters has been calculated and is presented graphically in Fig. III.

### EXPERIMENTAL SET UP FOR THE MEASUREMENT OF ELECTRIC FIELD COMPONENTS

The general experimental set up for the measurement of electric field components is shown in Fig. IV and Plate I, and is discussed below.

1. *Feed end of the guide*: A rectangular guide is excited in its dominant  $TE_{10}$  mode by 723 A/B klystron. Using a mode transformer this is converted to  $H_{11}$  mode in a circular guide. Since the field configuration of  $H_{11}$  mode in the circular guide is similar to that of the hybrid mode, the latter is excited by inserting the dielectric rod guide into the circular guide, the inserted end of the rod being tapered over  $3\lambda$  to ensure proper matching. As the diameter of the circular guide is more than that of the rod, a collar is used, which is gradually tapered over a length of  $3\lambda$  to the required diameter of the rod. The generator is isolated from the guide by an attenuator.

*Klystron Feed*: The klystron 723 A/B is mounted directly on the broadside of a rectangular waveguide, so that the output of the probe of the klystron protrudes through a hole made at the center of the broad face into the guide. This enables the excitation of the dominant  $TE_{10}$  mode in the rectangular guide. One end of the guide is fitted with an adjustable plunger. The plunger and the length of the output probe of klystron inside the guide are adjusted for maximum power transfer. The required voltages for the klystron is given by an electronically stabilized power supply. The reflector is modulated by 1000 c/s square wave.

*Mode Transformer*: The mode transformer is used to convert the dominant  $TE_{10}$  mode in a rectangular guide to the dominant  $H_{11}$  mode in a circular guide. The change of cross-section from rectangular to circular is brought about gradually over a length of  $3\lambda$  to ensure proper matching and maximum power transfer. The mode transformer is shown in Plate II.1.

*Collar*: The diameters of the dielectric rod guides that are used, are much smaller than that of the circular metal guide. Hence, to excite the dielectric rod in the hybrid mode, the diameter of the metal guide is reduced to the proper value required using appropriate collar. A collar is essentially a circular metal guide, gradually tapered to a lower diameter. The collars are shown in Plates II.2 to II.5.

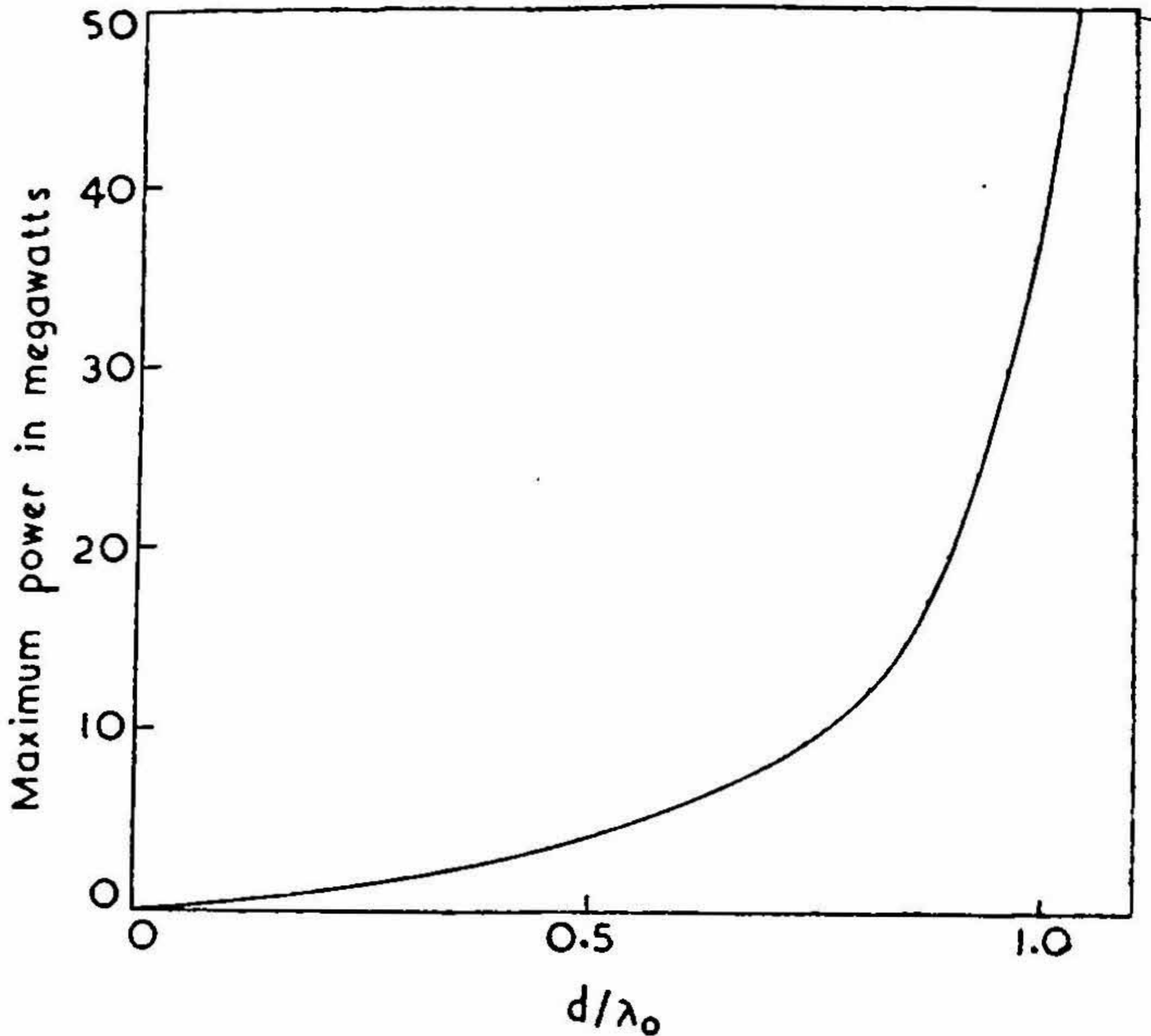


FIG. III

Maximum power carrying capacity of the dielectric rod waveguide excited in  $HE_{11}$  mode as a function of  $d/\lambda_0$ . ( $\bar{\epsilon}_1=2.6.$ ,  $\lambda_0=3.2$  cms.)

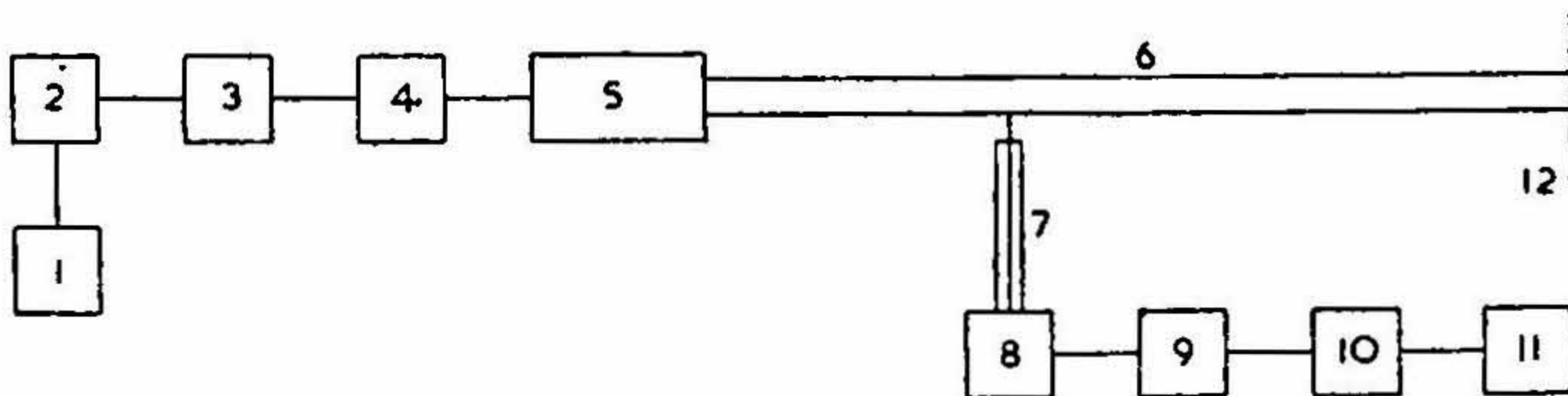


FIG. IV

Block Schematic diagram of experimental set up

- (1) Regulated power supply with square wave modulator. (2) Klystron, 723 A/B. (3) Variable attenuator, P.R.D. type 160. (4) Mode Transformer. (5) Guide collar. (6) Dielectric Rod guide. (7) Probe. (8) Coaxial to rectangular adapter. (9) Precision Attenuator, P.R.D. Type 185 B. (10) Broad band crystal mount, P.R.D. Type 612/A. (11) Detector Amplifier. (12) Shorting disc.

For lower diameters of the rod guide, it was found that the efficiency of launching is very poor. Hence in this case to improve the launching efficiency a dielectric collar is used. A dielectric rod of 1" diameter is taken and tapered to a point over a length of  $3\lambda$  on one side which is inserted into the metal guide. At the other end of the collar the diameter is gradually reduced to a required value and an axial hole is bored, into which the rod waveguide is inserted.

2. *The Free end of the guide*: The length of the guide is about 4' and the free end of the guide is shorted by a metal plate 1' in diameter as shown in the Plate III. The guide is suspended by means of nylon threads.

3. *Detector System*: The detecting system consists of a  $\lambda/4$  or  $\lambda/2$  probe connected through a precision attenuator (P.R.D. Type 185B) and a broad band crystal mount (P.R.D. Type 612A) to the detector amplifier. The probe along with the accessories is mounted on a probe carriage which has three independent, mutually perpendicular motions. The probe along with other accessories can be seen in the Plate III. The detector amplifier is a selective amplifier with a twin-tee tuned to 1 kc, the frequency of the square-wave with which the reflector voltage of the klystron is modulated.

#### MEASUREMENT OF ELECTRIC FIELD COMPONENTS

The probe is set parallel to the electric field component, that is being measured, close to the surface of the rod, almost touching the rod. The reflector voltage, the amplitude and the frequency of the square wave are tuned for the maximum detector reading. The crystal mount is tuned for the maximum. The attenuator is adjusted to some value so that the micrometer reads some low convenient value which is well above the noise reading of the detector amplifier. The position of the probe with respect to a scale provided is noted. The probe then is moved in steps of 1 mm and each time the attenuator is adjusted so as to get the same meter reading and the attenuator reading noted. The corresponding value of  $db$  is obtained from the calibration chart. A dipole probe is used for the measurement of  $E_z$  and a  $\lambda/4$  probe for the measurement of  $E_\rho$  and  $E_\phi$ . The measurements are done for rods of diameters 1",  $3/4$ " and  $1/2$ " at  $\lambda_0 = 3.2$  cms. The electric field components  $E_\rho$ ,  $E_\phi$  and  $E_z$  measured and normalized with respect to the surface value for different diameters are shown in the figures, V, VI and VII, along with the theoretical curves.

The guide wavelength is measured by moving the probe longitudinally parallel to the axis of the rod and taking the standing wave pattern. The guide wavelength obtained from the standing pattern is normalized with the free space wavelength and a plot of the graph  $\lambda_g/\lambda_0$  vs.  $d/\lambda_0$  is shown, along with the theoretical curve, in Fig. VIII.

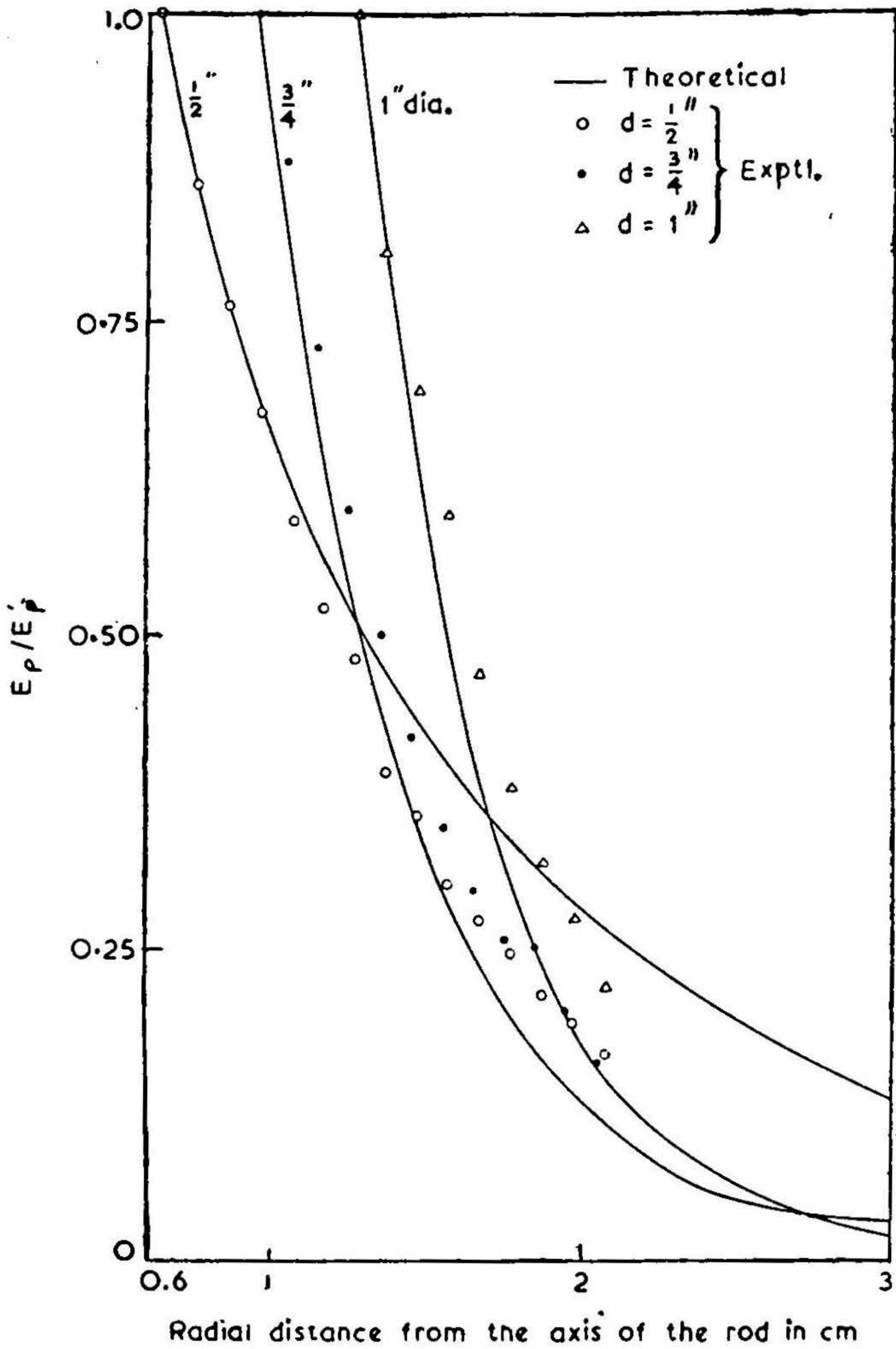


FIG. V

Variation of radial component,  $E_\rho$  of the electric Field with the radial distance,  $\rho$   
 [ $\bar{\epsilon}_1=2.6.$ ,  $\lambda_0=3.2$  cms.]  
 ( $E_\rho$  has been normalized with respect to its value  $E'_\rho$  on the surface of the rod)

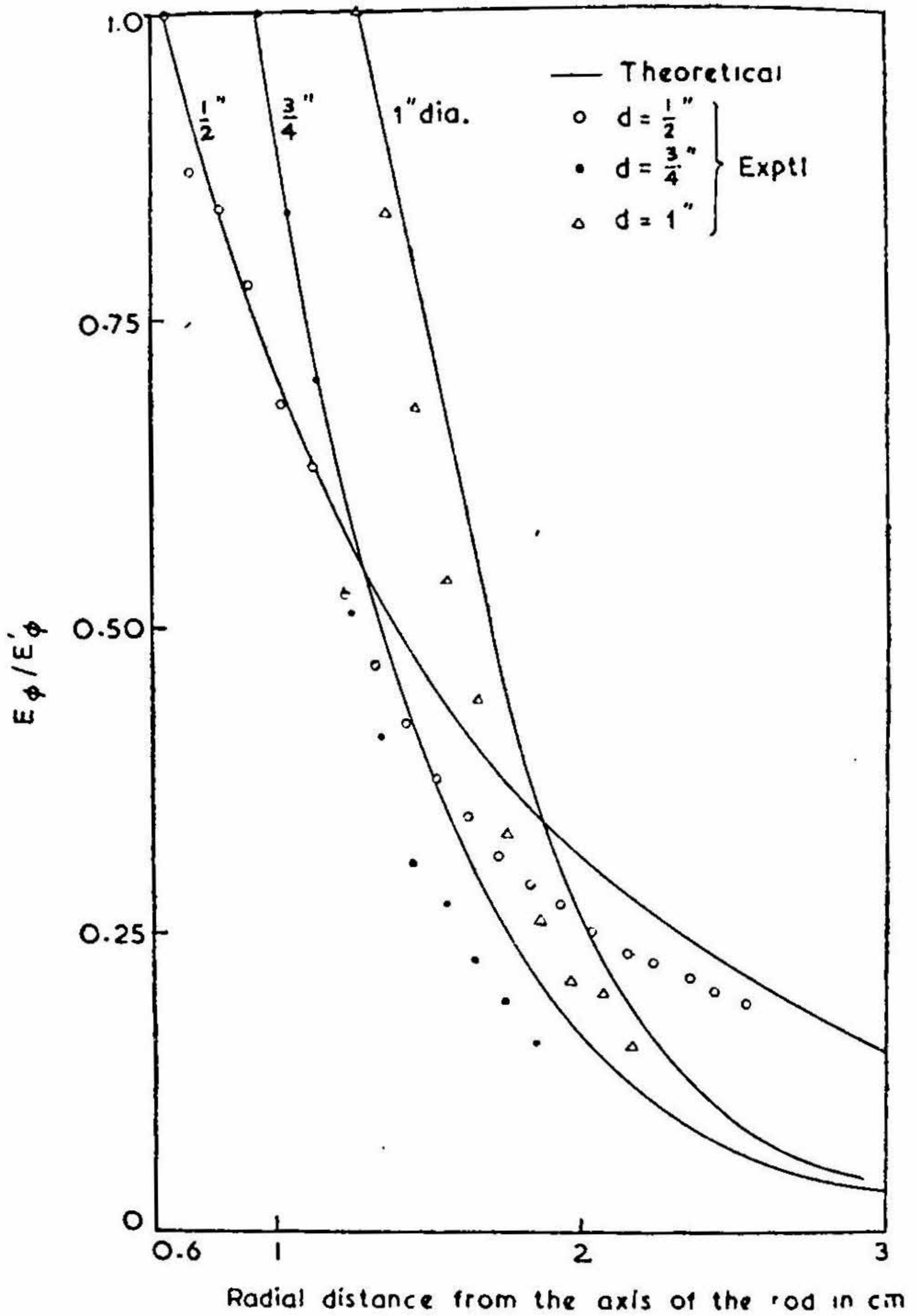


FIG. VI

Variation of the azimuthal component,  $E_\phi$  of the electric field with the radial distance,  $\rho$ .  
 ( $\bar{\epsilon}_1 = 2.6$ ,  $\lambda_0 = 3.2$  cms.)  
 ( $E_\phi$  has been normalized with respect to its value  $E'_\phi$  on the surface of the rod)

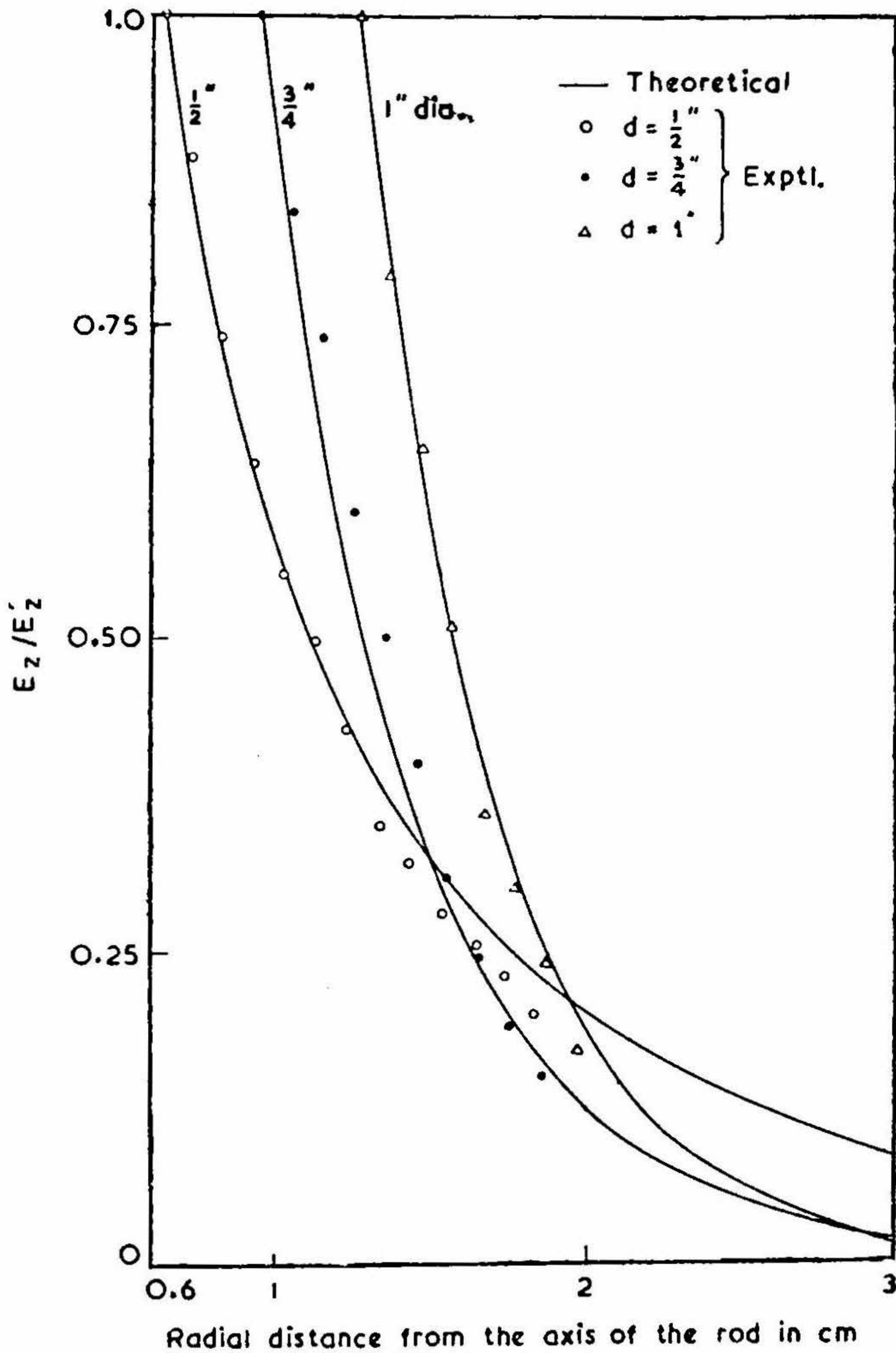


FIG. VII

Variation of the axial component,  $E_z$  of the electric field with the radial distance,  $\rho$ .

( $\bar{\epsilon}_1 = 2.6$ ,  $\lambda_0 = 3.2$  cms)

( $E_z$  has been normalized with respect to its value  $E'_z$  on the surface of the rod)

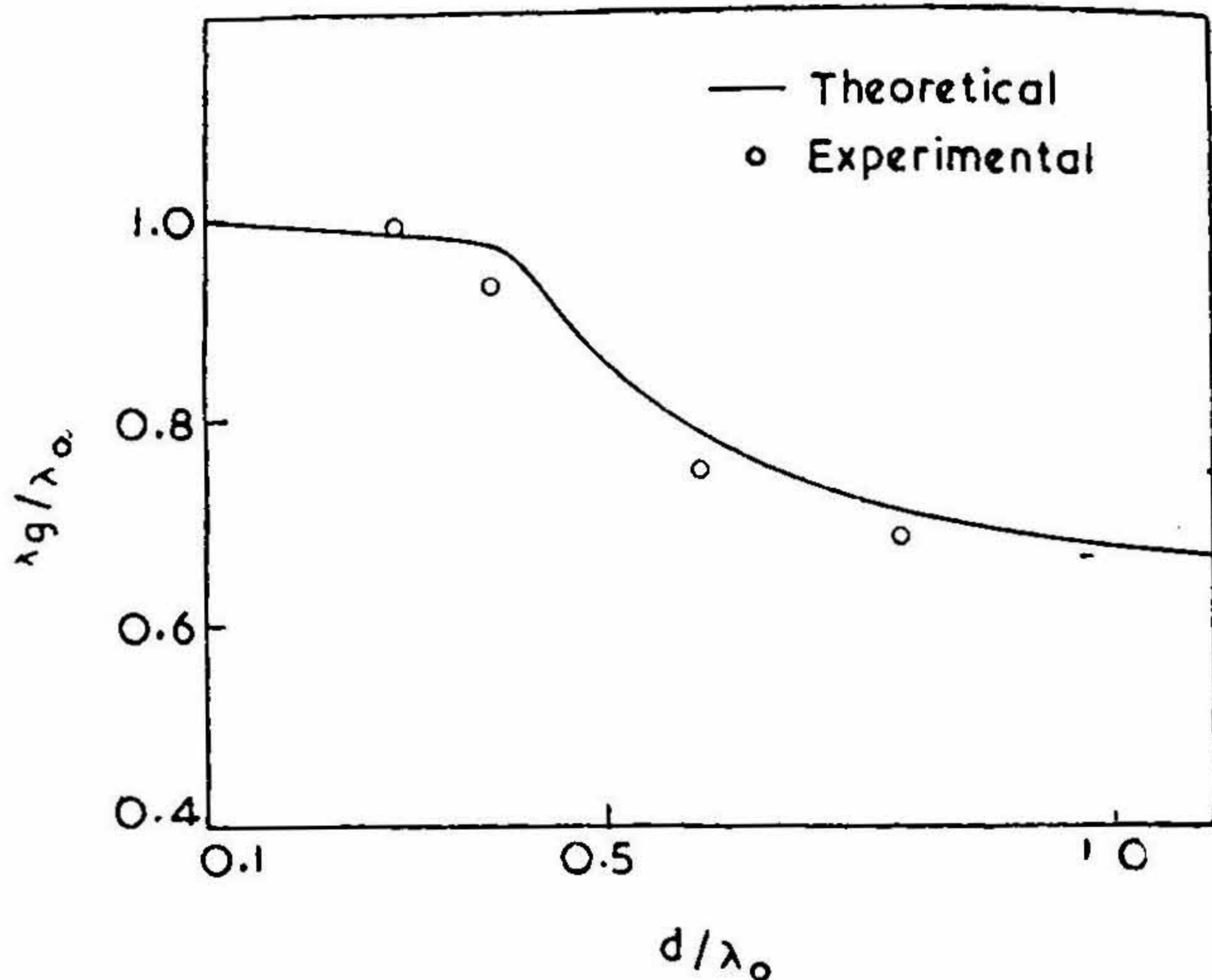


FIG. VIII

Variation of  $\lambda_g/\lambda_0$  with  $d/\lambda_0$ . 
$$\left(\frac{\lambda_g}{\lambda_0}\right)^2 = \frac{1}{\bar{\epsilon}_1 - x_1^2 (\lambda_0/\pi d)^2}$$
  
 ( $\bar{\epsilon}_1 = 2.6$ ,  $\lambda_0 = 3.2$  cms)

## DISCUSSION.

It is observed from the results that the power carrying capacities when the dielectric rod wave guide is excited by the E-modes are more than when it is excited by  $H$  or  $HE$  modes. It may be mentioned that in the case of metallic waveguide it has been shown<sup>4</sup> that the guide has the highest power carrying capacity when it is excited by E-modes.

The experimental results for the variation of  $\lambda_g/\lambda_0$  as a function of  $d/\lambda_0$  agrees favourably with that obtained by theory. It is seen from the figures V, VI and VII that there is fair agreement between theoretical and experimental results upto only small radial distances from the guide. The appreciable departure between the theory and experiment at larger radial distances from the guide remains to be explained.

## ACKNOWLEDGEMENT

The author expresses his thanks to Sri S. K. Chatterjee, for suggesting the problem and for guidance and to Dr. (Mrs.) R. Chatterjee for helpful discussions.

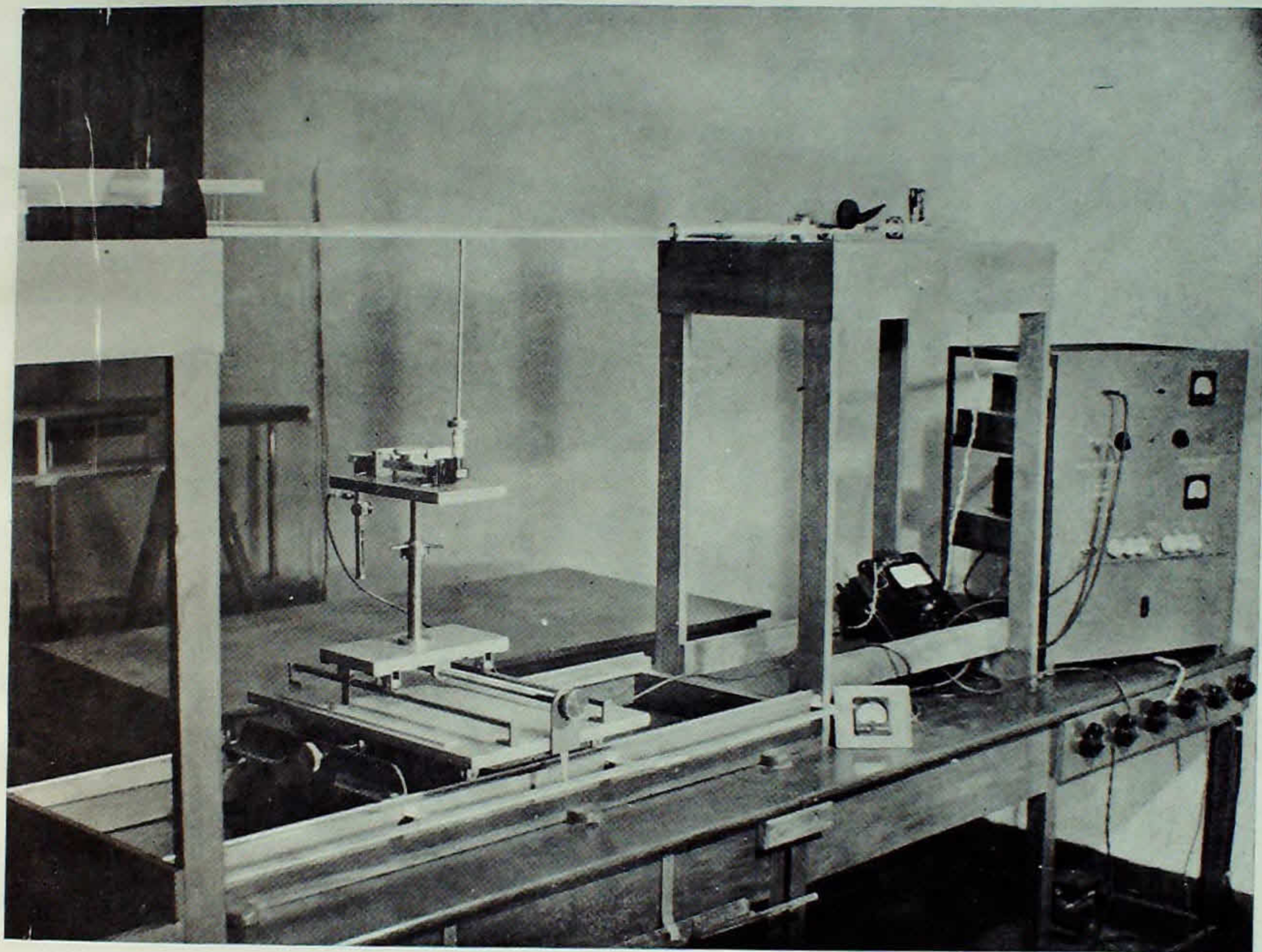


PLATE I

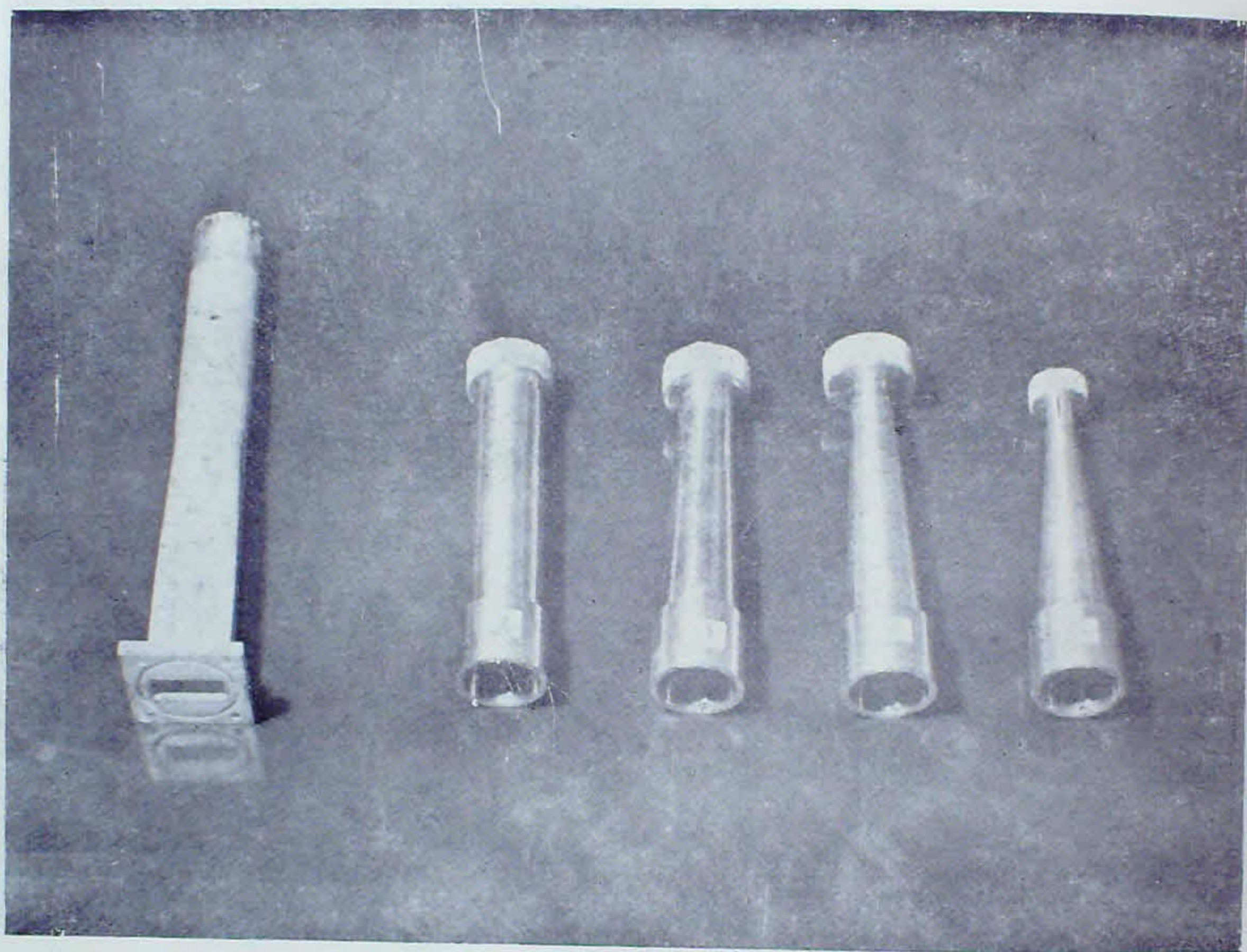


PLATE II

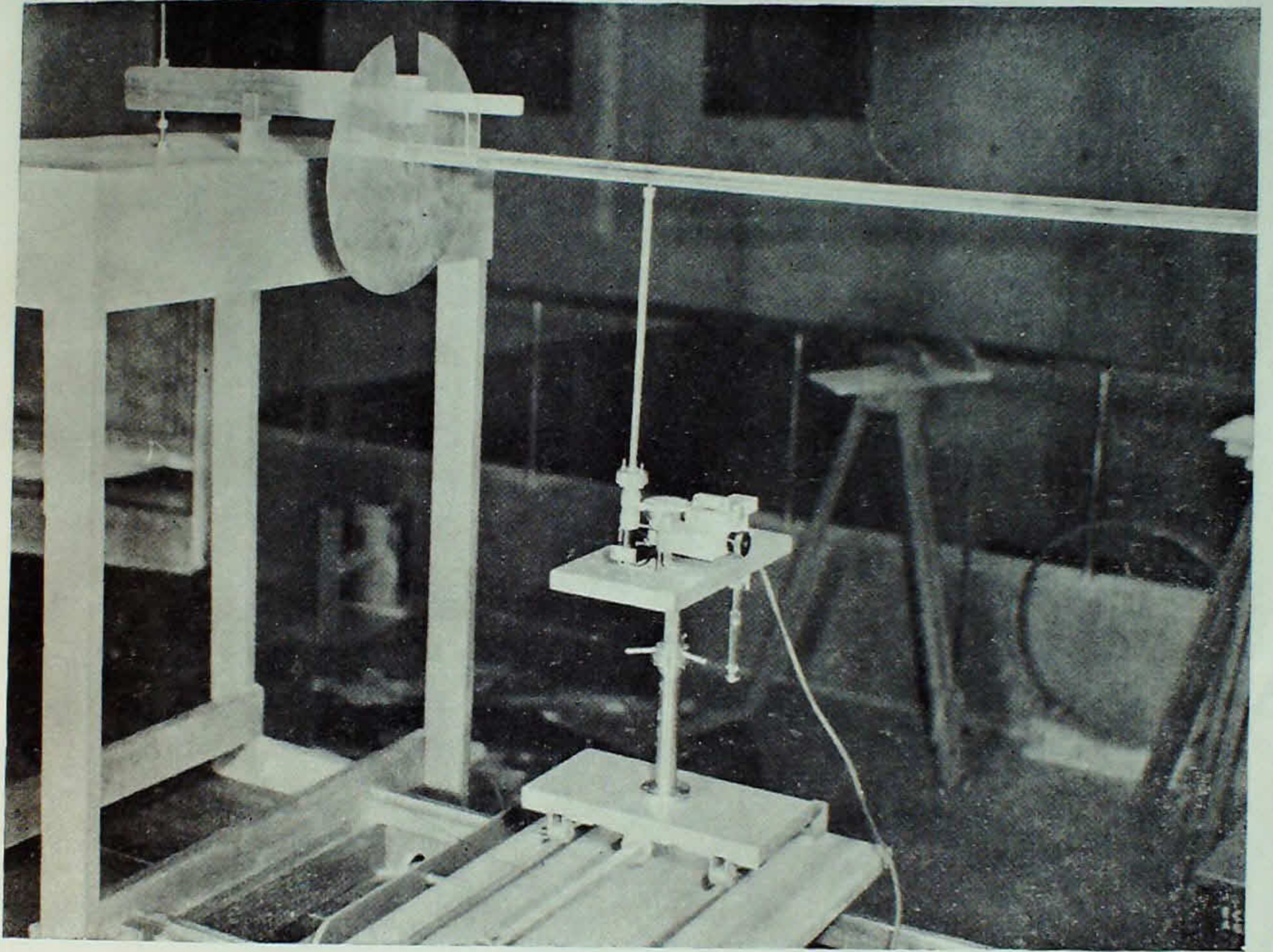


PLATE III

The author is grateful to Prof. S.V.C. Aiya, for the encouragement and facilities provided during the course of the work. The author also expresses his gratitude to the University Grants Commission for the award of a Fellowship ; to the Secretary, Birla Educational Trust., Dr. S. M. Mitra, Principal, Birla College, Pilani for granting study leave.

REFERENCES

1. Keily, D. G.                   ...           ...    " Dielectric aerials ", *Methuen Monograph*.
2. Subramaniam, V.           ...           ...    *J. Indian Inst. Sci.*, 1962, 44, 4.
3. Cooper, R.                   ...           ...    *Jour. I.E.E.*, 1947, 94, Part III.
4. Barlow, H. M.               ...           ...    *Proc. I.E.E.*, 1952, 99, Part III.